

Vibration Energy Harvesting

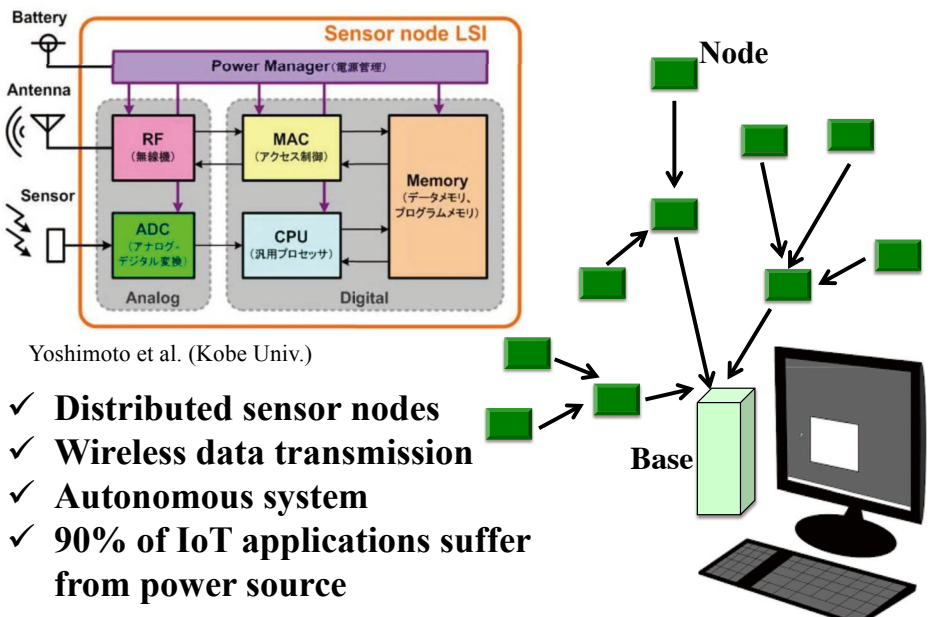
Professor Yuji Suzuki

Department of Mechanical Engineering
The University of Tokyo, Japan
e-mail: ysuzuki@mesl.t.u-tokyo.ac.jp



東京大学
THE UNIVERSITY OF TOKYO

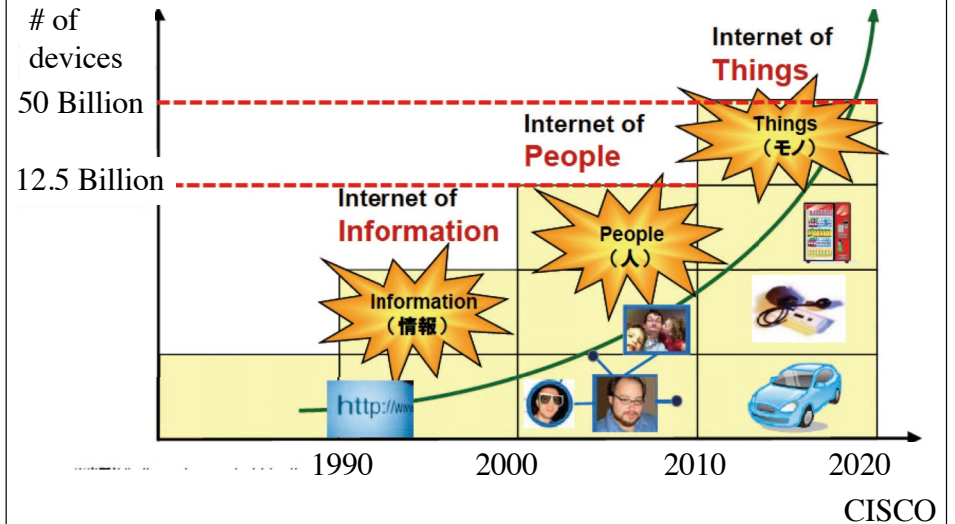
Wireless Sensor Network/IoT/M2M



Yuji Suzuki, The University of Tokyo

Internet of Things (IoT)

Network among various objects in daily life



Why Wireless?

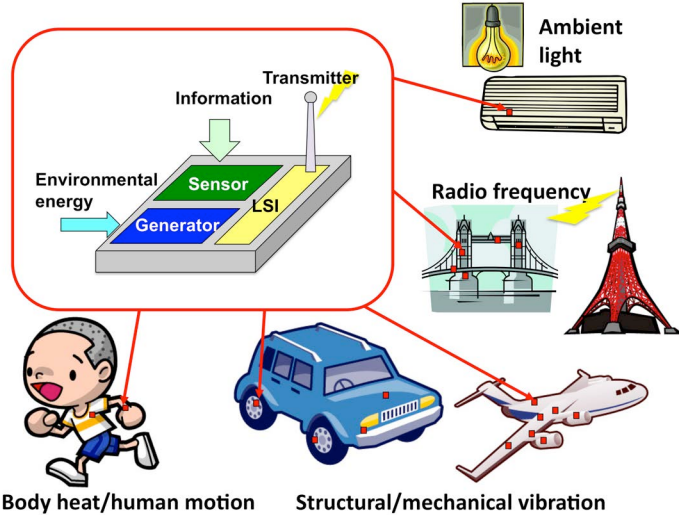
- ✓ Cables are expensive and/or heavy.
- ✓ After market
- ✓ Maintenance free

Issue: How to supply power?

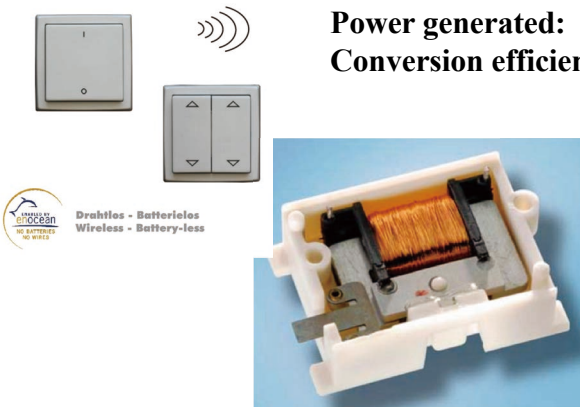


Energy Harvesting

Extract electricity from environmental energy source for low-power-consumption electronics



EnOcean: Power Generation Switch



Zumtobel Spain / Luxmate
55 floors, 223 m
4,200 light/blind switches

... Installed in 250,000 buildings in Europe

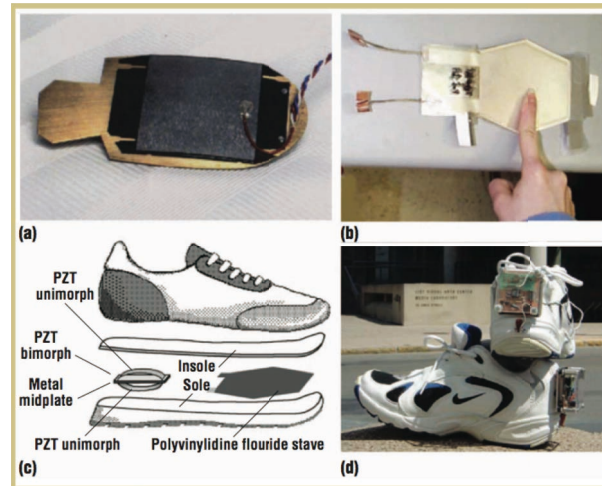


Power generated:
Conversion efficiency:

350 μ J
4.7 %

Power Generation from Heel Strike

1998 Parasitic Power Harvesting in Shoes, J. Kymmissis (MIT)



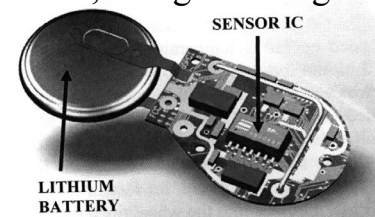
8.3 mW (MIT)

Paradiso & Starner (2005)

Tire Pressure Monitoring Sensor (TPMS)

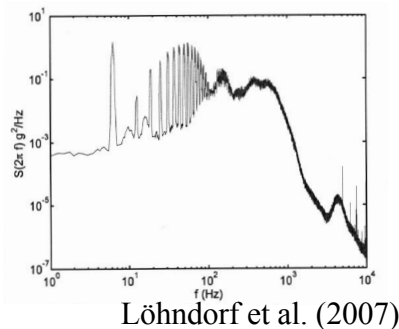
TREAD Act.

To avoid tire burst, tire wear, low gas mileage



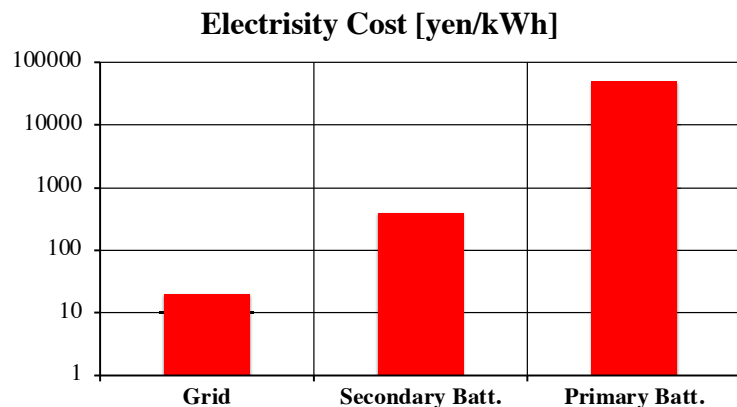
Specification:

- 1 Transmission/min.
- Power required: 1.2mJ=20 μ W



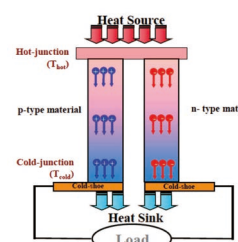
Löhndorf et al. (2007)

High-added-value Energy Source



Mobile energy source has high added value.

Thermoelectric Generator

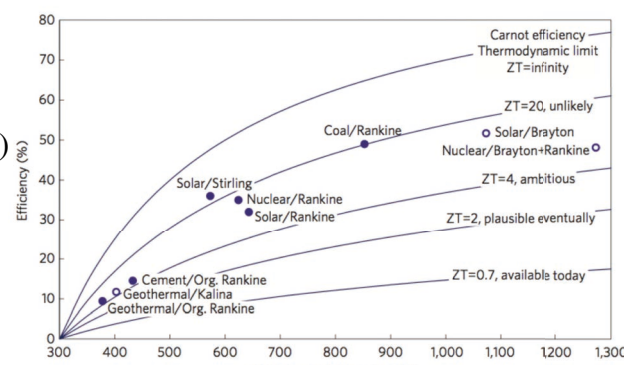


$$ZT = \frac{\sigma S^2}{\lambda} T$$

$$\eta_{\max} = \frac{Carnot}{TE\ Materials} = \frac{T_{hot} - T_{cold}}{T_{hot}} \cdot \frac{\sqrt{1+ZT} - 1}{\sqrt{1+ZT} + \frac{T_{cold}}{T_{hot}}}$$

$\sigma \sim 10^4 - 10^6 \text{ } \Omega^{-1} \text{ m}^{-1}$
(metal – semiconductor)

$S > 0.1 \text{ } \mu\text{V/K}$
(semiconductor)
 $\lambda \sim 1 \text{ W/(m K)}$
(glass)



Vining (2009)

Roadmap for Energy Harvesting

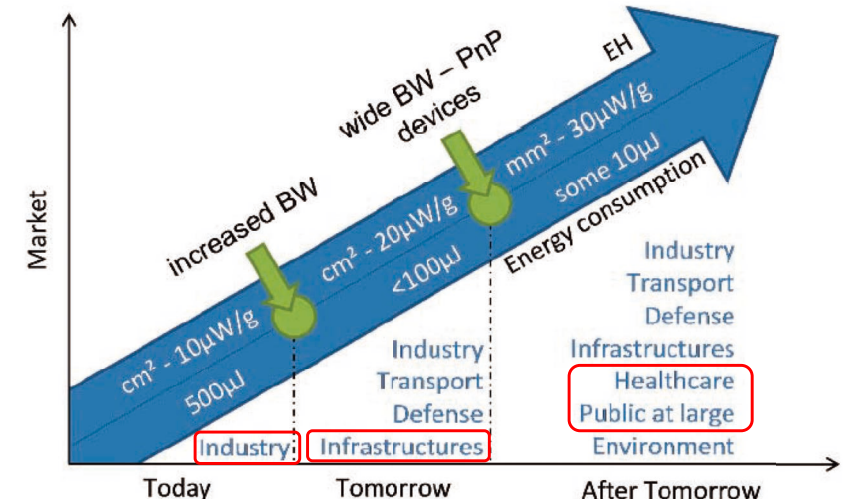


Figure 21 Roadmap for vibration energy harvesters (Source: CEA-Leti)

IERC

Structural Health Monitoring System for Aircraft

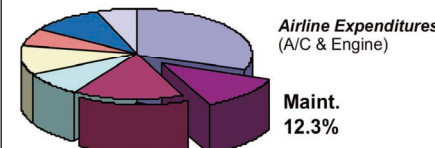
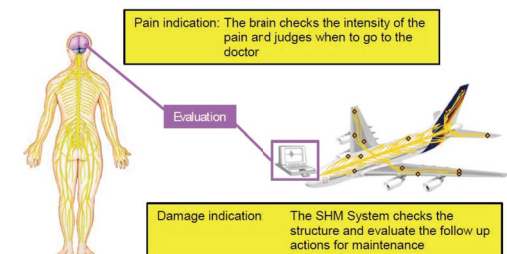
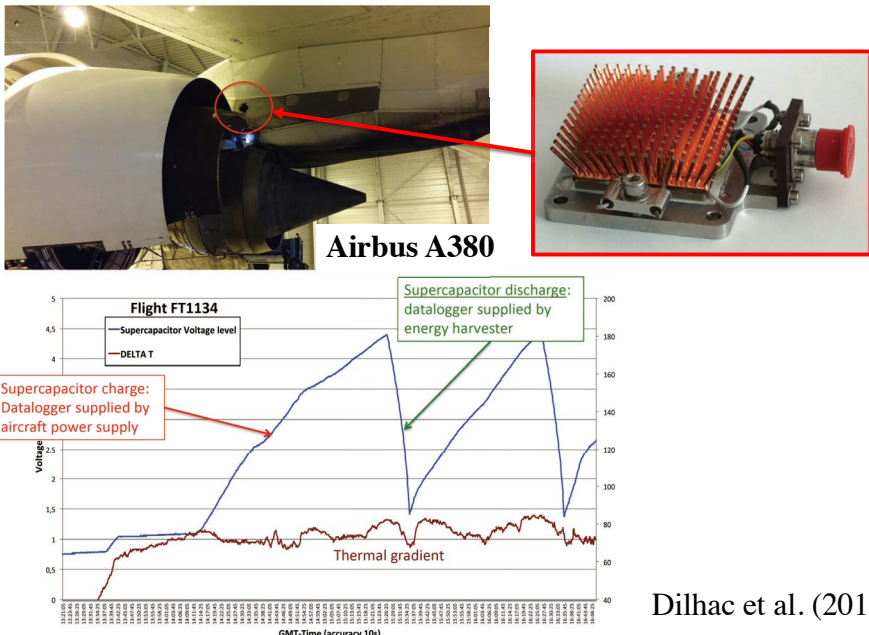


Figure 1: Maintenance cost

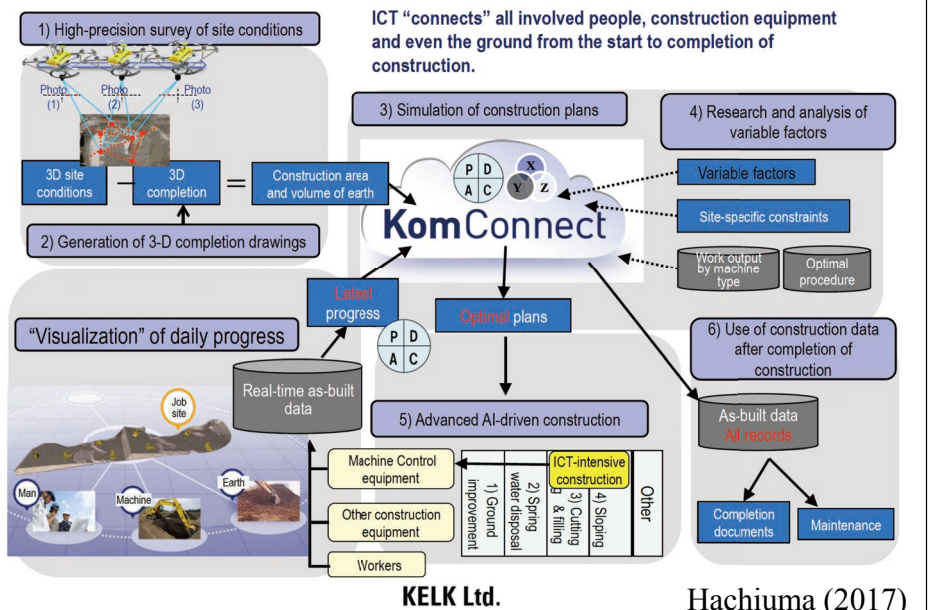


- Wireless sensor needed
- Long-term use (>20 years)
- Severe temperature variation

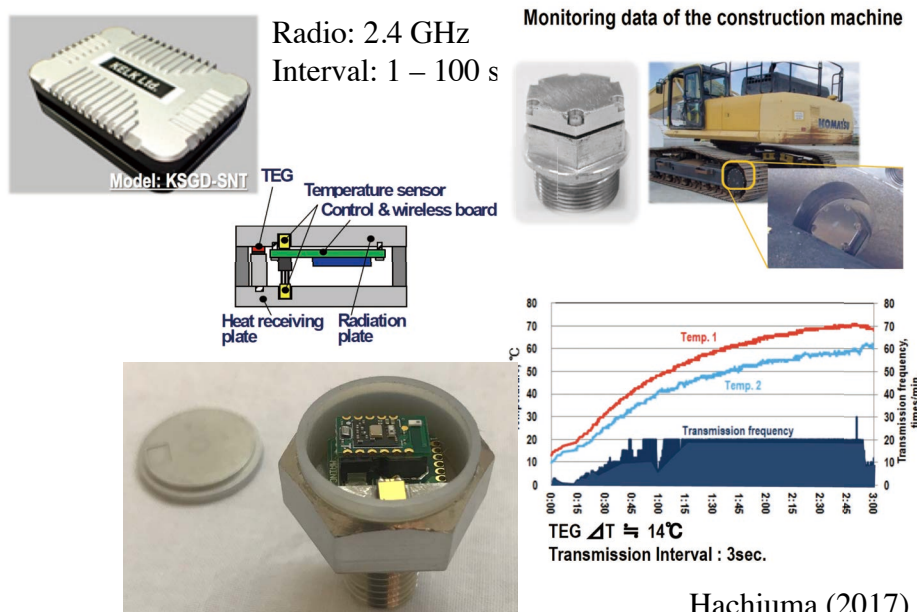
Wireless Sensor on Aircraft



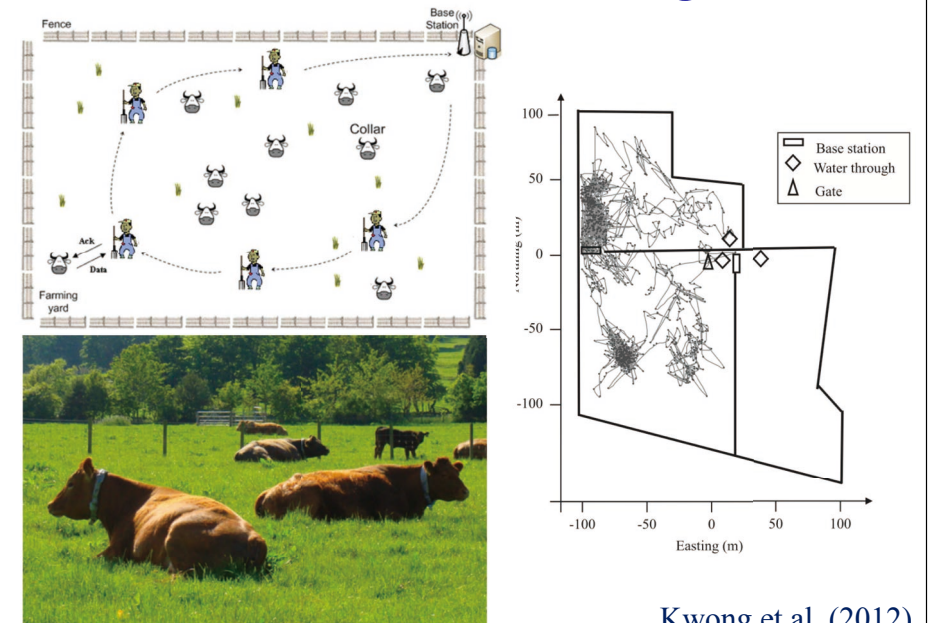
SMART CONSTRUCTION



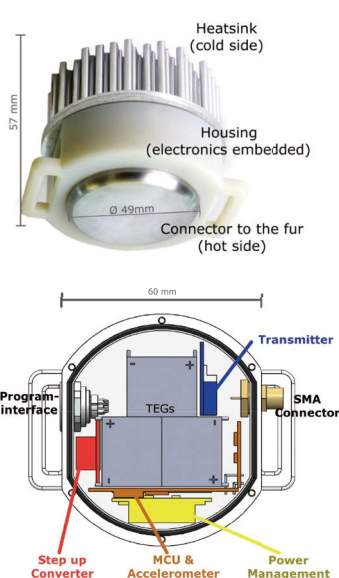
TEG Wireless Sensor Module (KELK)



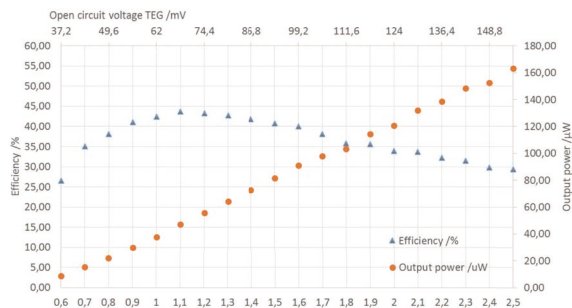
Livestock Monitoring



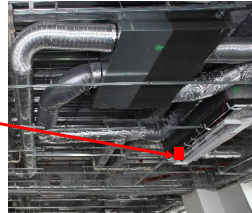
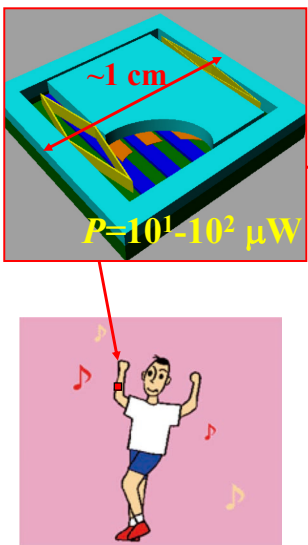
Battery-less VHF-Beacon for Mammals



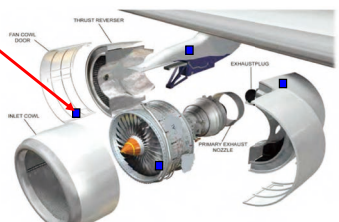
Baumker et al.
(2018)



Vibration Energy Harvesting (EH)



Air flow
fluctuation,
piping vibration
BEMS/HEMS



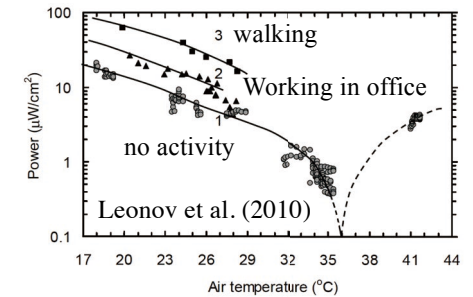
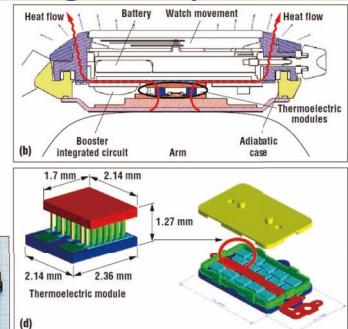
50 Hz @
Take-off

Automotive/Aviation
Tire pressure monitoring (TPMS)
Structural health monitoring (SHM)

Human/Animal motion
Biomedical, Agriculture

Thermal EH Using Body Heat

SEIKO
Thermic



Mechanical Model of Energy Harvester

$$m\ddot{x} + c_d\dot{x} + kx = my_0\omega^2 \cos\omega t$$

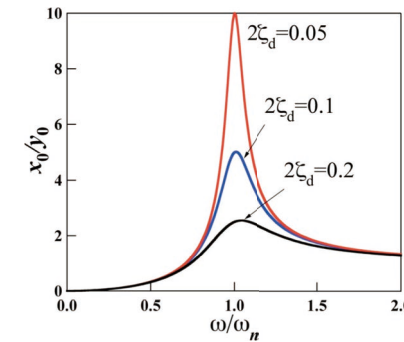
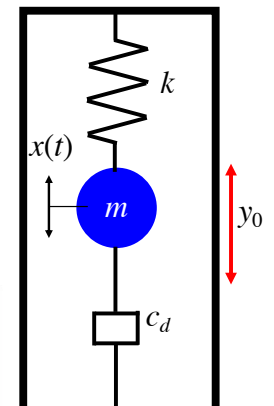
$$\omega_n = \sqrt{\frac{k}{m}}, \zeta_d = \frac{c_d}{2m\omega_n}, \omega_c = \frac{\omega}{\omega_n}$$

$$x(t) = \frac{y_0\omega^2}{\sqrt{(1-\omega_c^2)^2 + \{2\zeta_d\omega_c\}^2}} \cos(\omega t - \phi)$$

When $\omega_c = 1$

$$x_{\max} = \frac{y_0}{2\zeta_d}$$

$$Q_d \equiv \frac{x_{\max}}{y_0} = \frac{1}{2\zeta_d}$$



Mechanical Model of Energy Harvester

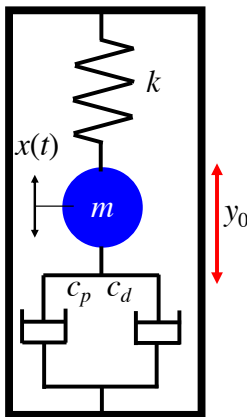
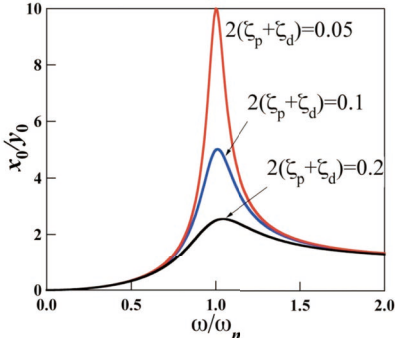
$$m\ddot{x} + (c_d + c_p)\dot{x} + kx = my_0\omega^2 \cos \omega t$$

$$\omega_n = \sqrt{\frac{k}{m}}, \zeta_d = \frac{c_d}{2m\omega_n}, \zeta_p = \frac{c_p}{2m\omega_n}, \omega_c = \frac{\omega}{\omega_n}$$

$$x(t) = \frac{y_0\omega_c^2}{\sqrt{(1-\omega_c^2)^2 + \{2(\zeta_d + \zeta_p)\omega_c\}^2}} \cos(\omega t - \phi)$$

When $\omega_c = 1$

$$x_{\max} = \frac{y_0}{2(\zeta_d + \zeta_p)}$$



Mechanical Model of Energy Harvester

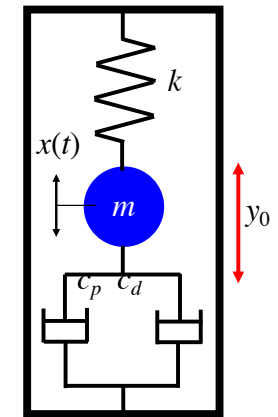
External Work = Output Power + Loss

$$P = \int F_p \dot{x} dt = \int c_p \dot{x}^2 dt \\ = \frac{m\zeta_p y_0^2 \omega_c^3 \omega^3}{(1-\omega_c^2)^2 + \{2(\zeta_d + \zeta_p)\omega_c\}^2}$$

Optimization of ζ_p ($dP/d\zeta_p = 0$)

$$\zeta_p = \sqrt{\zeta_d^2 + \frac{(1-\omega_c^2)^2}{4\omega_c^2}}$$

$$P_{opt} = \frac{my_0^2 \omega_c^3 \omega^3 \sqrt{\zeta_d^2 + \frac{(1-\omega_c^2)^2}{4\omega_c^2}}}{(1-\omega_c^2)^2 + 4\omega_c^2 \left\{ \sqrt{\zeta_d^2 + \frac{(1-\omega_c^2)^2}{4\omega_c^2}} + \zeta_d \right\}^2}$$



Mechanical Model of Energy Harvester

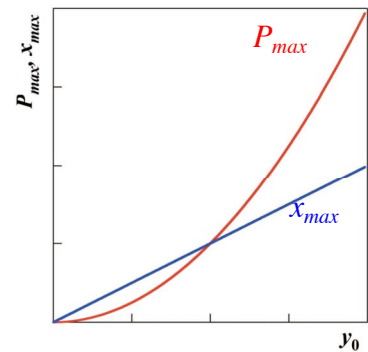
$$P_{opt} = \frac{my_0^2 \omega_c^3 \omega^3 \sqrt{\zeta_d^2 + \frac{(1-\omega_c^2)^2}{4\omega_c^2}}}{(1-\omega_c^2)^2 + 4\omega_c^2 \left\{ \sqrt{\zeta_d^2 + \frac{(1-\omega_c^2)^2}{4\omega_c^2}} + \zeta_d \right\}^2}$$

At resonance ($\omega_c=1$),

$$\zeta_p = \sqrt{\zeta_d^2 + \frac{(1-\omega_c^2)^2}{4\omega_c^2}} = \zeta_d$$

$$P_{\max} = \frac{my_0^2 \omega_c^3}{16\zeta_d}, x_{\max} = \frac{y_0}{2(\zeta_d + \zeta_p)} = \frac{y_0}{4\zeta_d}$$

Conversion Efficiency: $\eta = 50\%$

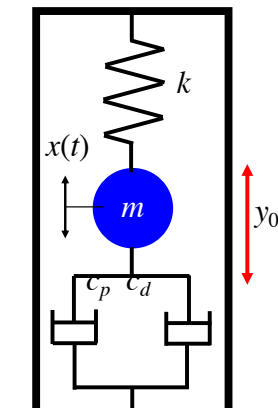


Mechanical Model of Energy Harvester

If the mass amplitude is limited by x_{\lim} ,

$$\zeta_p = \frac{1}{2\omega_c} \sqrt{\omega_c^4 \left(\frac{y_0}{x_{\lim}} \right)^2 - (1-\omega_c^2)^2} - \zeta_d \\ = \frac{1}{2} \cdot \frac{y_0}{x_{\lim}} - \zeta_d$$

$$P = \frac{m\zeta_p y_0^2 \omega_c^3 \omega^3}{(1-\omega_c^2)^2 + \{2(\zeta_d + \zeta_p)\omega_c\}^2} \\ = \frac{1}{2} m\omega_n^3 y_0 x_{\lim} \left(1 - \zeta_d \frac{2x_{\lim}}{y_0} \right) \\ = \frac{1}{2} m\omega_n^3 y_0 x_{\lim} \left(1 - \frac{x_{\lim}}{y_0} \cdot \frac{1}{Q_d} \right), \quad \eta = \frac{y_0 / x_{\lim} - 2\zeta_d}{y_0 / x_{\lim}} \geq 50\%$$



Mechanical Limit of Energy Harvester

$$m\ddot{x} + (c_d + c_p)\dot{x} + kx = mx_0\omega^2 \cos\omega t$$

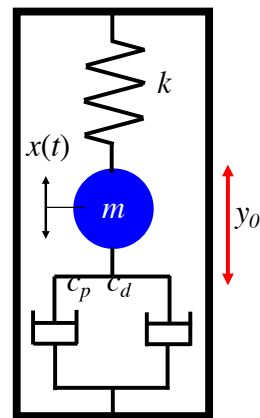
$$\omega_n = \sqrt{\frac{m}{k}}, \zeta = \frac{c_d + c_p}{2\sqrt{mk}}, \omega_c = \frac{\omega}{\omega_n}$$

$$x(t) = \frac{\omega_c^2}{\sqrt{(1-\omega_c^2)^2 + (2\zeta\omega_c)^2}} x_0 \cos(\omega t - \phi)$$

$$P = \int c_p \dot{x}^2 dt = \frac{c_p}{2} \frac{\omega_c^4}{(1-\omega_c^2)^2 + (2\zeta\omega_c)^2} \omega^2 x_0^2$$

$$P_{\max} = \frac{1}{2} m y_0 \omega_n^3 x_{\max}$$

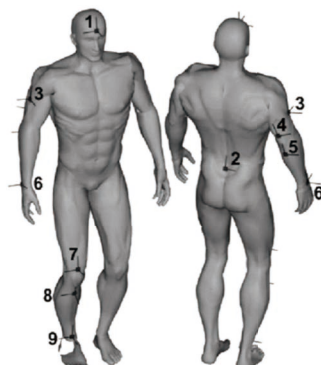
VDRG limit



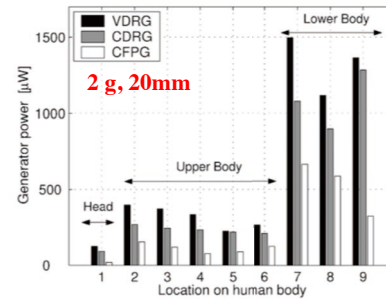
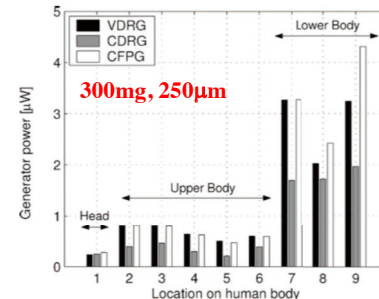
Mitcheson et al. (2004)

x_{\max} : Maximum traveling distance of mass

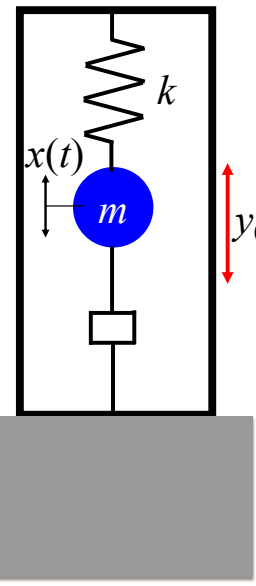
Evaluation of Output Power



Buren et al. (2006)



Mechanical Limit of Vibration EH



Energy Flow (2-step conversion)
Vibration energy in environment
 1st step \downarrow **M→M**
Kinetic energy of mass
 2nd step \downarrow **M→E**
Electricity

VDRG limit (Mitcheson et al., 2004)

$$P_{\max} = \frac{1}{2} m y_0 \omega_n^3 x_{\max}$$

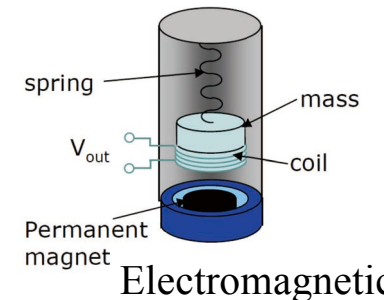
m : mass, ω_n : Resonant freq.

y_0 : External amplitude

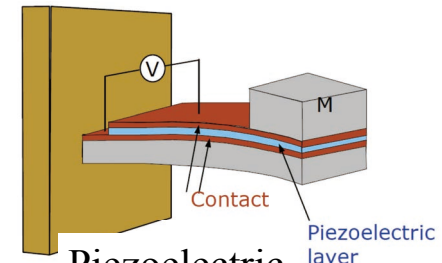
x_{\max} : Max. traveling distance

20 Hz, 1 G
200 g, 1 cm
 for 1W

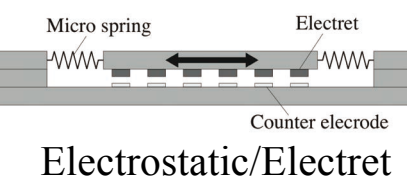
Mechanical-Electrical Energy Conversion



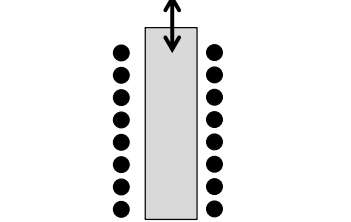
Electromagnetic



Piezoelectric

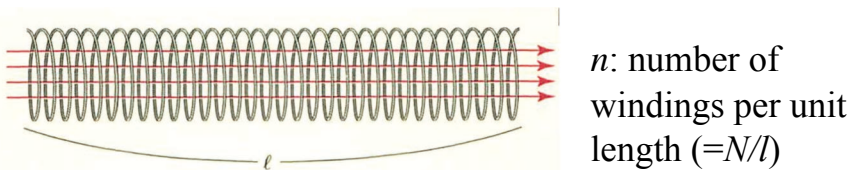


Electrostatic/Electret



Inverse
Magnetostrictive

Energy Density of Electromagnetic



Ampere's law $B = \mu_0 n I$
Magnetic flux $\Phi = \mu_0 n I A$

$$V = -N \frac{d\Phi}{dt} = -\mu_0 n^2 A \ell \frac{dI}{dt}$$

$$L = \mu_0 n^2 A \ell$$

$$W = \frac{1}{2} L I^2 / A \ell = \frac{1}{2 \mu_0} B^2$$

Damping Force in Electromagnetic

Induced Voltage $V(t) = NAB' \dot{x}$, $B' = \frac{dB}{dx}$
Number of winding: N , Area: A , B

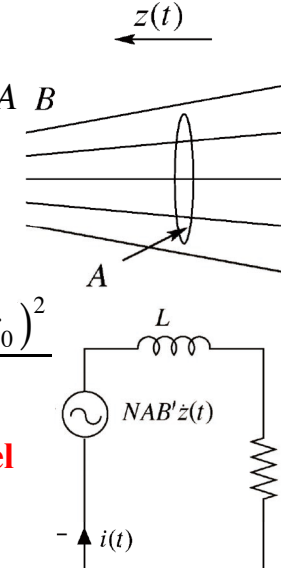
Peak Current $I_0 = \frac{\omega NAB' x_0}{\sqrt{R^2 + \omega^2 L^2}}$

Output Power

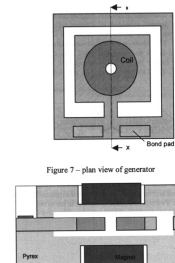
$$P = \frac{I_0^2 R}{2} = \frac{R^2}{2(R^2 + \omega^2 L^2)} \cdot \frac{(\omega NAB' x_0)^2}{R}$$

$$P \sim c_p \dot{x}^2 = c_p (\omega x_0)^2 \quad \text{VDRG Model}$$

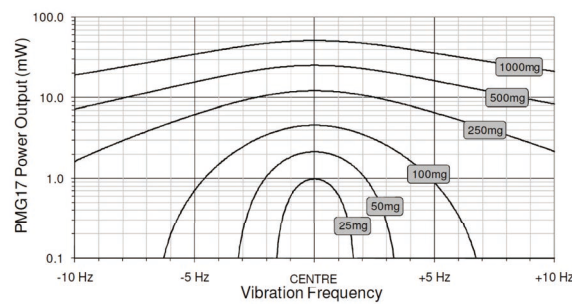
$$\therefore c_p = \frac{R^2}{2(R^2 + \omega^2 L^2)} \cdot \frac{(NAB')^2}{R}$$



Perpetuum Ltd. (UK)



Electromagnetic
PMG-17
1 mW@100Hz, 25mg
φ55mm, 655g
www.perpetuum.com



A PLANAR ELECTROMAGNETIC VIBRATION ENERGY HARVESTER WITH A HALBACH ARRAY

Dibin Zhu*, S. P. Beeby, M. J. Tudor and N. R. Harris

School of Electronics and Computer Science, University of Southampton, Southampton, UK

*Presenting Author: dz@soton.ac.uk

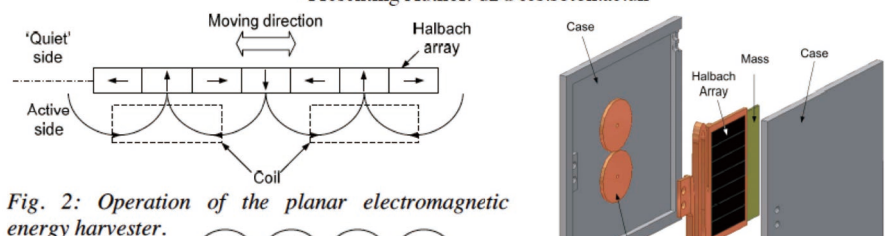


Fig. 2: Operation of the planar electromagnetic energy harvester.

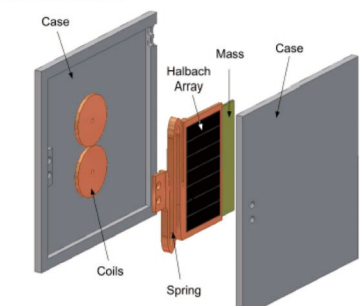


Fig. 1: The planar electromagnetic energy harvester.
Table 1. Comparisons of magnetic field strength.

		Magnetic field strength (T)
Halbach array	Active side	0.14
	'Quiet' side	0.016
Normal layout		0.09

PowerMEMS 2011 × 2

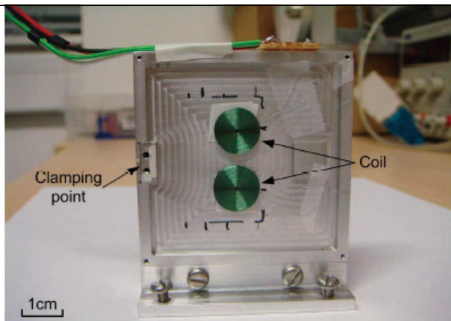


Fig. 6. Base of the energy harvester.

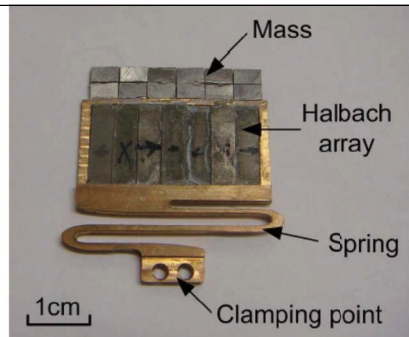


Fig. 7. Resonator with Halbach Array.

Table 2: Output voltage at various acceleration levels.

Acceleration (mg)	100	200	300
Resonant frequency (Hz)	44.9	44.9	44.8
RMS voltage (V)	.27	0.54	0.79
Peak voltage (V)	0.38	0.76	1.12
Normalized voltage	1	2	2.9

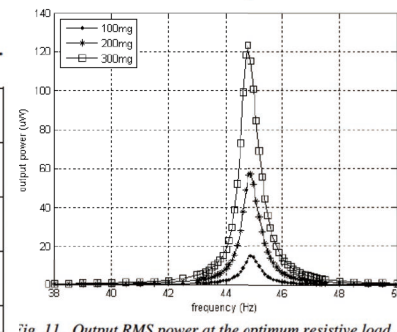


Fig. 11. Output RMS power at the optimum resistive load.

Analysis of Piezoelectric EH

$$\begin{cases} M\ddot{u} + C\dot{u} + K_E u + \alpha V = F \\ I = \alpha \dot{u} - C_0 \dot{V} \end{cases}$$

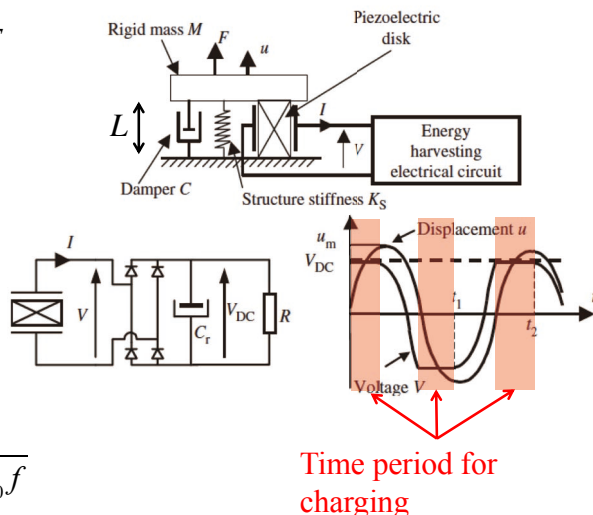
$$\alpha = \frac{e_{33} A}{L}$$

$$\int_{t_1}^{t_2} I dt = \frac{V_{DC}}{R} \frac{T}{2}$$

$$V_{DC} = \frac{R \alpha f}{1/4 + R C_0 f} u_m$$

$$P_{max} = \frac{\alpha^2 f}{C_0} u_m^2, R_{opt} = \frac{1}{4 C_0 f}$$

f : frequency, C_0 : capacitance, u_m : amplitude



Lefevre et al. (2005)

Energy Density of Piezoelectric (d_{33})

$$Q = d_{33} \times T \times w \times b$$

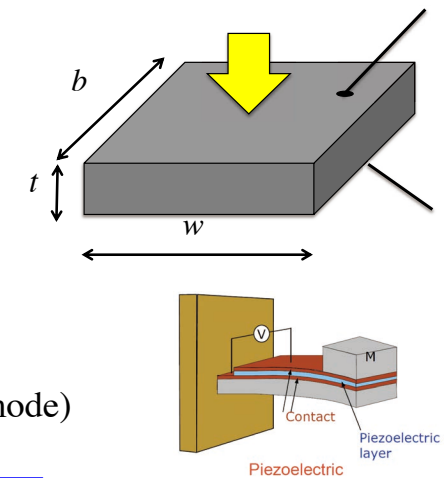
$$C = \varepsilon_{33}^T \frac{wb}{t}$$

$$V = \frac{Q}{C} = \frac{d_{33} T t}{\varepsilon_{33}^T}$$

$$W = \frac{1}{2} C V^2 / wbt = \frac{1}{2} \frac{d_{33}^2 T^2}{\varepsilon_{33}^T}$$

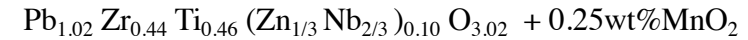
$$FoM = d_{33}^2 / \varepsilon_{33}^T \text{ (same for } d_{31} \text{ mode)}$$

$T \uparrow, d_{33} \uparrow \text{ and } \varepsilon_{33} \downarrow \text{ for higher } W$

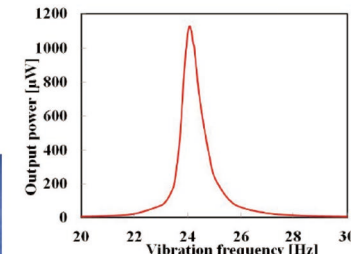


In general, heavy tip mass required for lowering the resonant frequency.

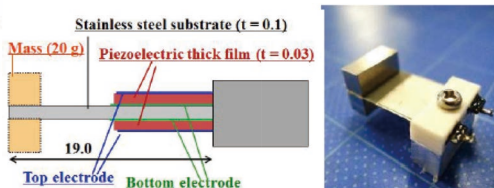
Screen-printed PZT on SUS Cantilever



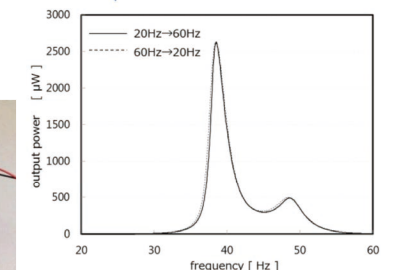
	Thick film	bulk
$\varepsilon_{33}^T / \varepsilon_0$	400	1400
d_{31}	-45 pm/V	-115 pm/V
k_{31}	0.20	0.30



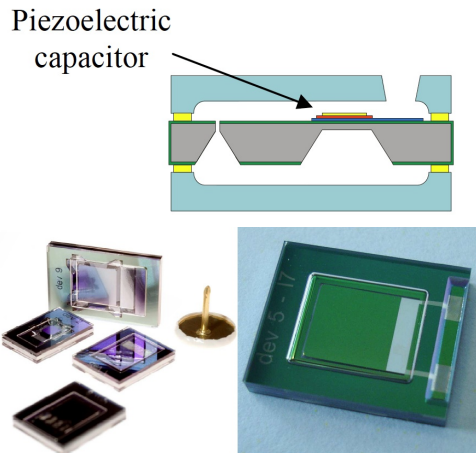
$P_{max}=1.1 \text{ mW @ 24 Hz, 0.1 G}$



Oishi et al.,
PowerMEMS 2014

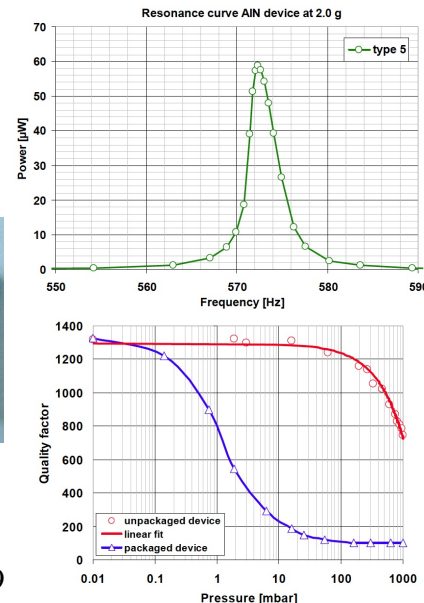


AlN-based Piezoelectric EH (IMEC-NL)

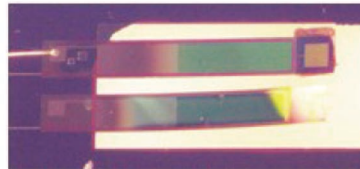


Mass: 3 x 3 mm²
 $P_{\max} = 0.27 \mu\text{W}$ (air) @ 1G
 $= 32 \mu\text{W}$ (vacuum) @ 1G

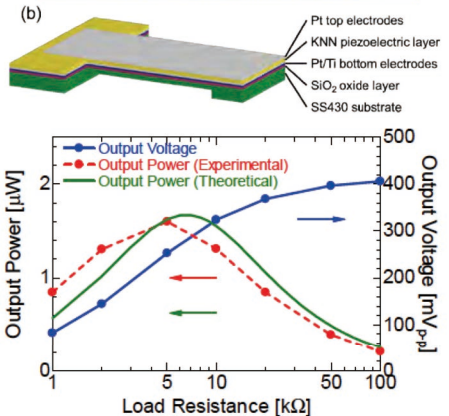
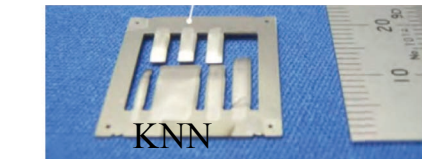
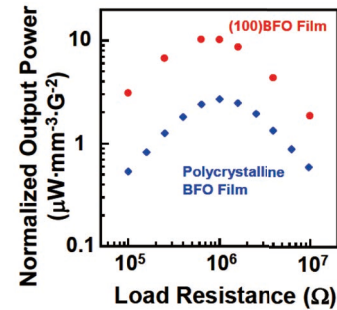
Elfrink et al., PowerMEMS 2008, 2009



Vibration EH with Non-lead Piezoelectric Material



1 mm
 \longleftrightarrow
BiFeO₃



Murakami et al., PowerMEMS 2013

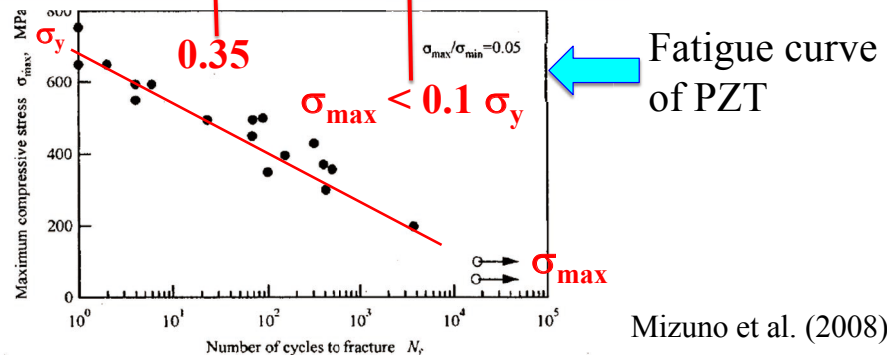
Tsujiura et al. (2013)

Power Density of Generators

- Optimistic estimate for piezoelectric ...

Type	Energy density (mJ cm ⁻³)	Equation	Assumptions
Piezoelectric	35.4	$(1/2)\sigma_y^2 k^2 / c$	PZT 5 H
Electromagnetic	24	$(1/2)B^2 \mu_0$	0.25 T
Electrostatic	4	$(1/2)\epsilon_0 E^2$	$3 \times 10^7 \text{ V m}^{-1}$

Roundy & Wright (2004)
 σ_y : Yield stress



Mizuno et al. (2008)

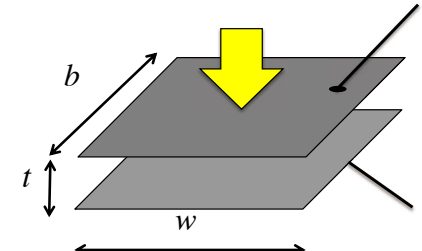
Energy Density of Electrostatic

$$Q = CV$$

$$C = \epsilon \epsilon_0 \frac{wb}{t}$$

$$W = \frac{1}{2} CV^2 / wbt$$

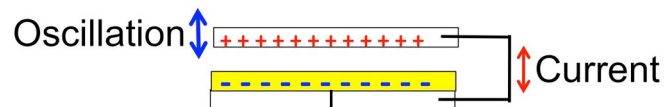
$$= \frac{1}{2} \epsilon \epsilon_0 \frac{V^2}{t^2} = \frac{1}{2} \epsilon \epsilon_0 E^2$$



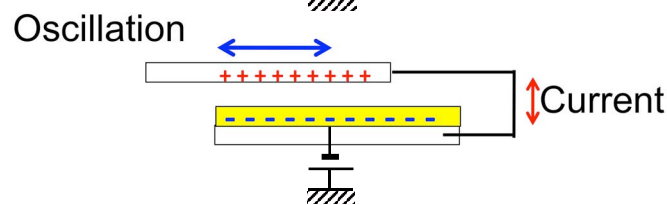
ϵ, E should be higher for higher W .

Different Configurations of Electrostatic Generator

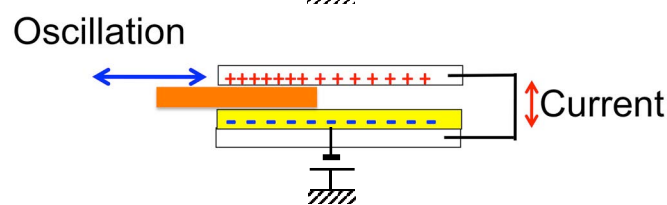
Gap-closing



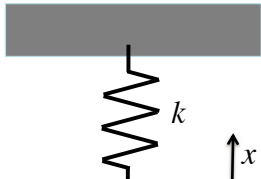
Overlapping-area change



Permittivity change



Pull-In Phenomena



$$J = \frac{1}{2}CV^2, \quad F_e(x) = -\frac{dJ}{dx} = \frac{\varepsilon\varepsilon_0AV^2}{2x^2}$$

$$F_{net} = k(x_0 - x) - \frac{\varepsilon\varepsilon_0AV^2}{2x^2} = 0$$

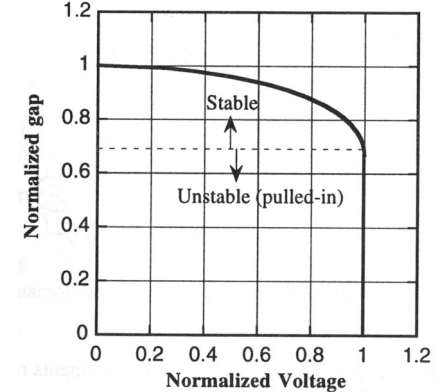


$$\delta F_{net} = \left(-k + \frac{\varepsilon\varepsilon_0AV^2}{x^3} \right) \delta x$$

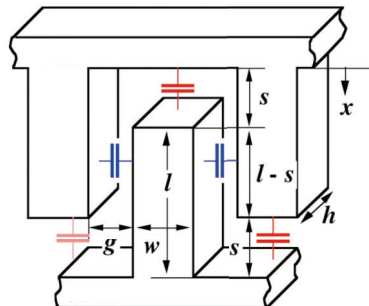
For stability,

$$\delta F_{net} > 0 \text{ for } \delta x < 0$$

$$x_{PI} = x_0 - \frac{\varepsilon\varepsilon_0AV^2}{2kx_{PI}^2} = \frac{2}{3}x_0$$



Comb Drive with Overlapping-Area Change



$$F = \varepsilon_0 \left\{ \frac{wg}{(s-x)^2} + 1 \right\} \frac{Wh}{g(w+g)} V^2$$

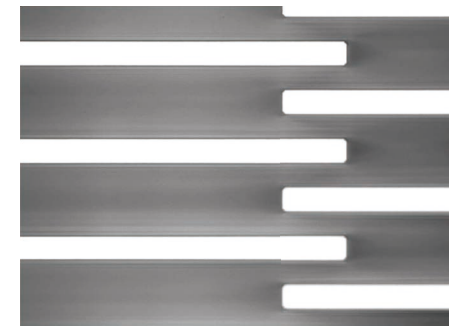
$$\text{When } \frac{w}{s}, \frac{g}{s} \ll 1$$

$$F = \varepsilon_0 \frac{Wh}{g(w+g)} V^2$$

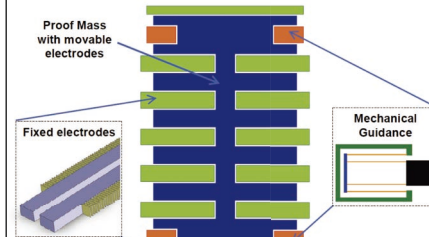
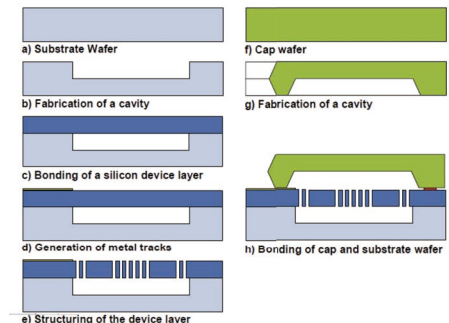
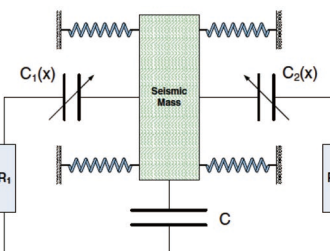
$$C_{tip} = \varepsilon_0 \frac{wh}{s-x}$$

$$C_{side} = \varepsilon_0 \frac{(l-s+x)h}{g}$$

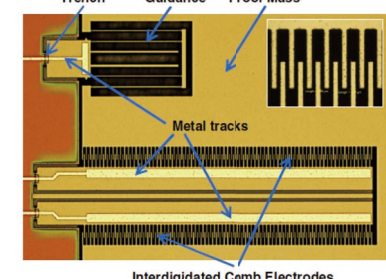
$$C = N \left\{ 2\varepsilon_0 \frac{wh}{s-x} + 2\varepsilon_0 \frac{(l-s+x)h}{g} \right\}$$

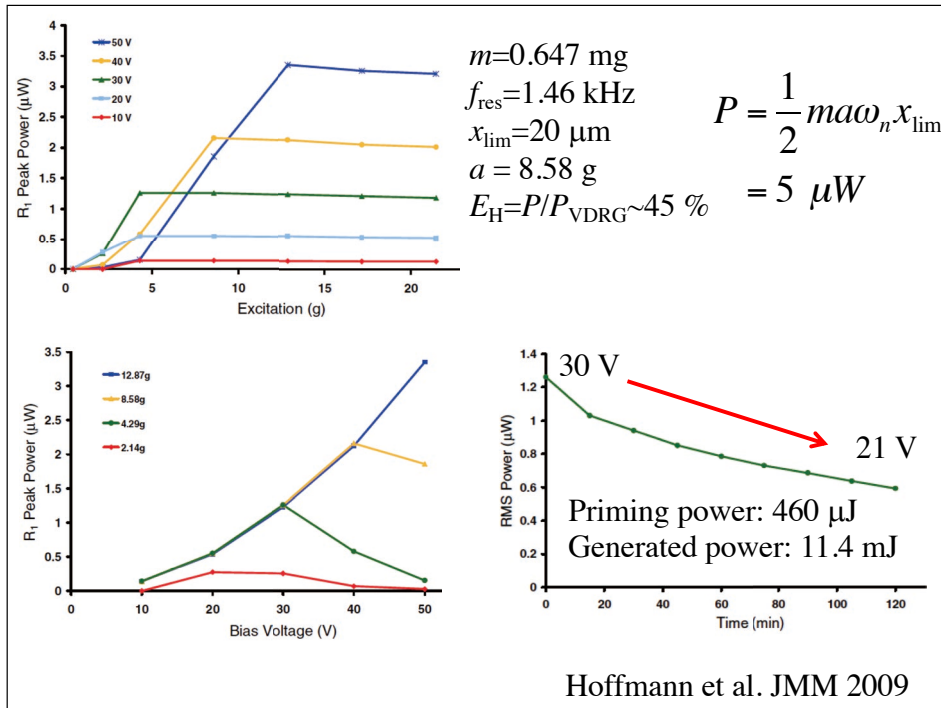


MEMS Electrostatic Generator with Comb Drives



Device layer thickness 50 μm
Hoffmann et al. JMM 2009





Short History of Electret/Electret Generator

1925 Mototaro Eguchi (Imperial Naval Research Lab)
Carnauba wax, Thermal charging method

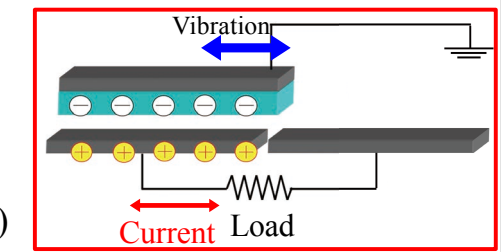


1960 Gerhard Sessler (Bell Lab → Darmstadt U.)
Foil electret microphone



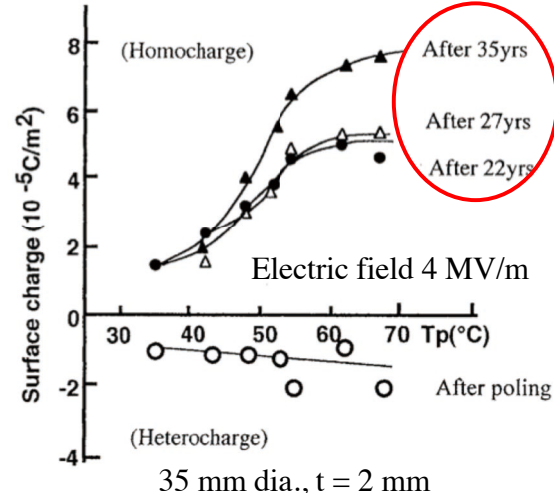
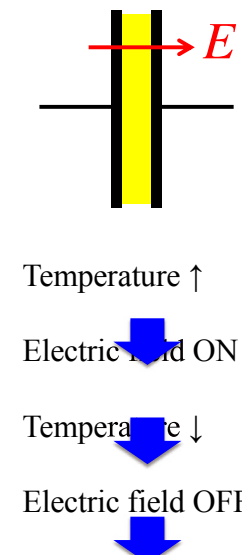
1978 O. D. Jefimenko
Rotational electret generator

1990's Y. Tada
1 mW@5,000 rpm
with PTFE electret



2003 J. Boland et al.
First MEMS electret
generator (Teflon AF)

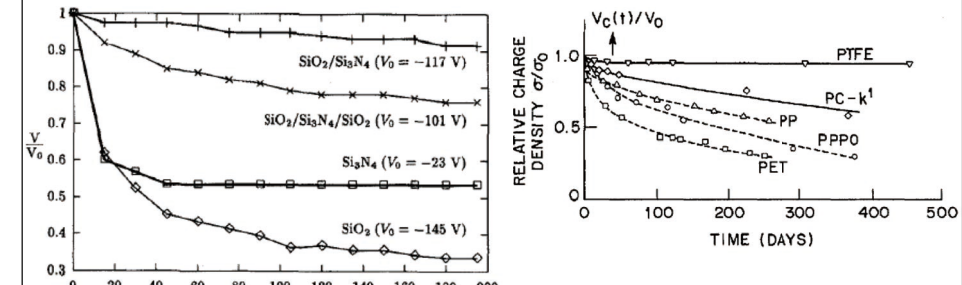
Thermal Charging of Carnauba Wax



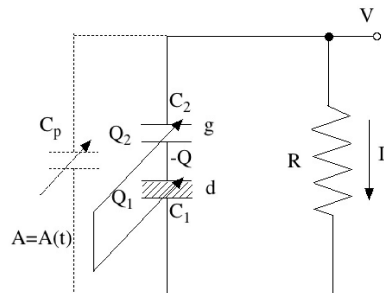
Takamatsu (1992)

Electret Materials

	Inorganic Material	Fluorinated Polymer
Surface charge density	++	+
Thermal stability of charges	++	+/-
Long-term stability of charges	-	++
Fabrication ease	+/-	++



Capacitor Model of Electret Generator

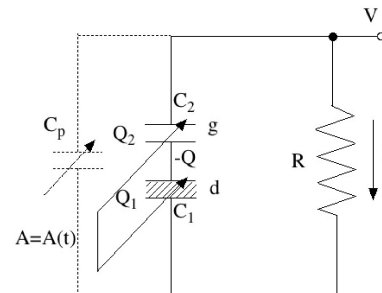


σ: Surface charge density
f: Frequency[Hz]
d: Thickness of electret
g: Air gap
n: Number of pole
A: Overlapping area

$$\begin{cases} V = -\frac{Q_1}{C_1} + \frac{Q_2}{C_2} \\ C_1 = \frac{\epsilon \epsilon_0}{d} A(t), \quad C_2 = \frac{\epsilon_0}{g} A(t) \\ Q = Q_1 + Q_2 \\ I = -\frac{dQ_2}{dt}, \quad V = IR \end{cases}$$

$$P = \frac{\sigma^2 d^2 R}{\left\{ \epsilon \epsilon_0 R + \frac{1}{nA_0 f} (\epsilon g + d) \right\}^2}$$

Capacitor Model of Electret Generator



σ: Surface charge density
f: Frequency[Hz]
d: Thickness of electret
g: Air gap
A₀: Area of electret

$$V = \frac{\sigma d}{2\epsilon \epsilon_0} \quad R_{\max} = \frac{1}{\epsilon_0 n A_0 f} \left(g + \frac{d}{\epsilon} \right)$$

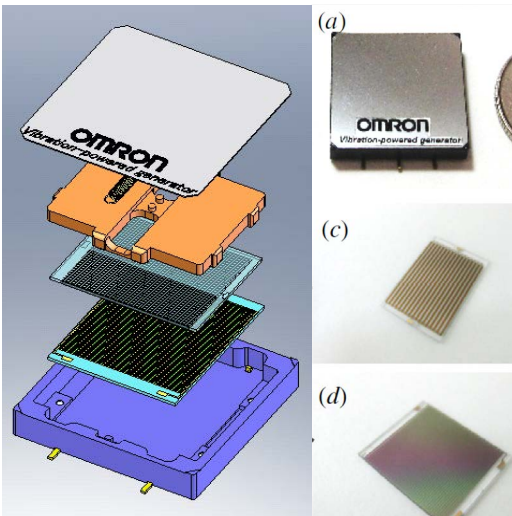
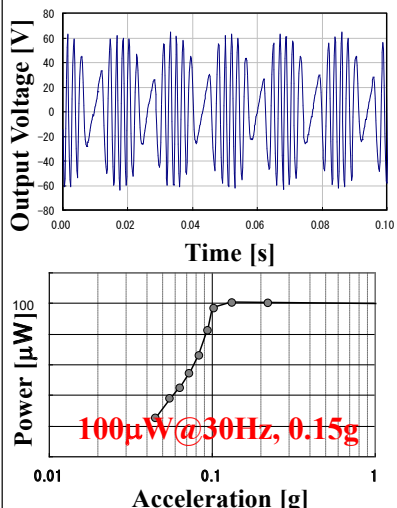
$$P_{\max} = \frac{\sigma^2 \cdot n A_0 f}{4 \frac{\epsilon \epsilon_0}{d} \left(\frac{\epsilon g}{d} + 1 \right)}$$

↔

Power Electromagnetic $P \sim (Af)^2$
 Electrostatic $P \sim Af$
 (Af)

Miniature Electret Generator (OMRON)

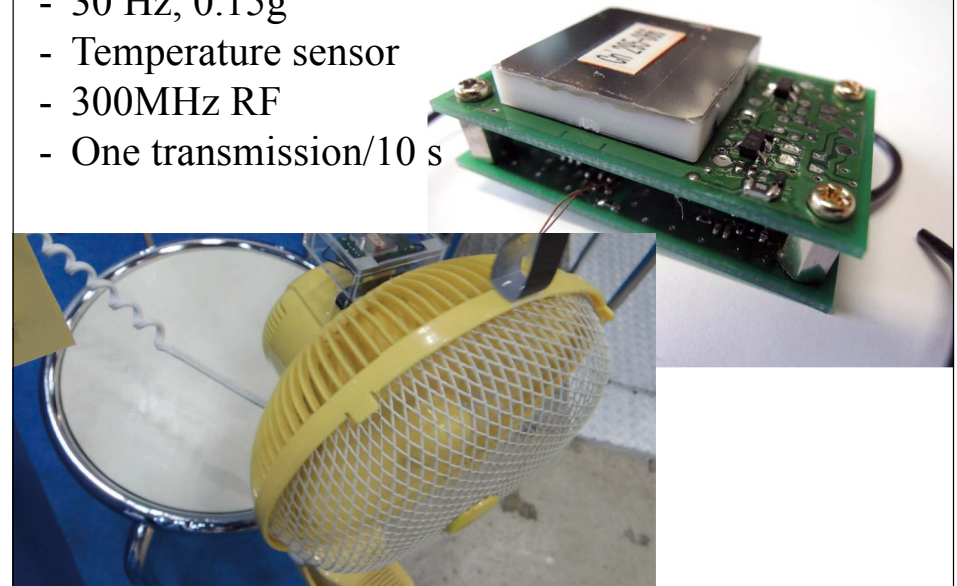
20 x 20 x 4 mm (1.6 cm³), Weight: 3.7 g, $E_H \sim 20\%$
CYTOP EGG Electret



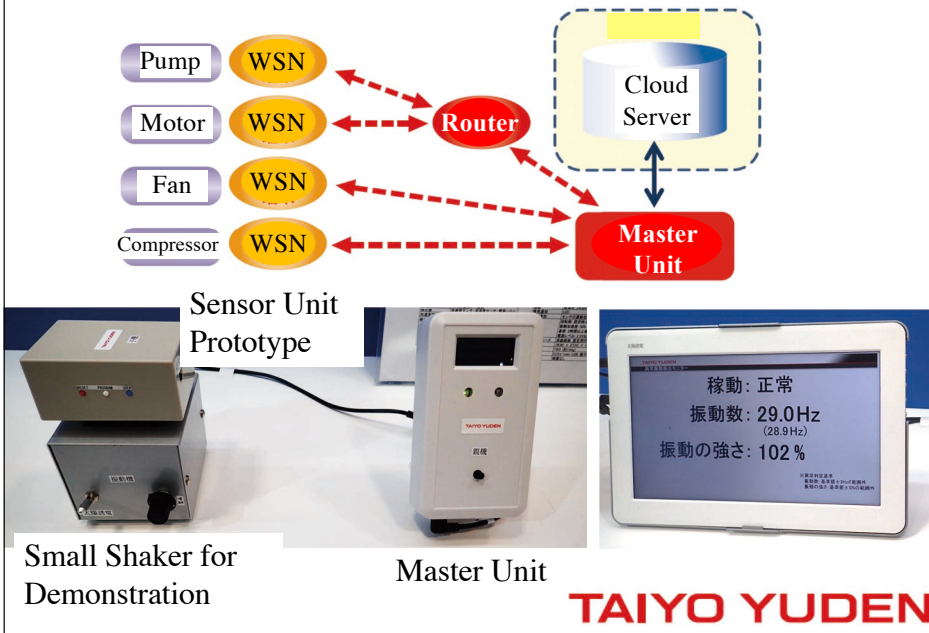
Masaki et al. JMM 2011

RF Sensor Module with Electret EH

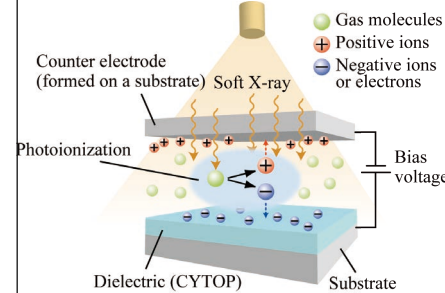
- 30 Hz, 0.15g
- Temperature sensor
- 300MHz RF
- One transmission/10 s



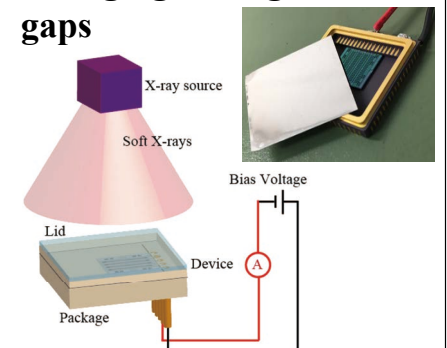
Early Failure Detection for Rotational Machines



Soft X-ray Charging



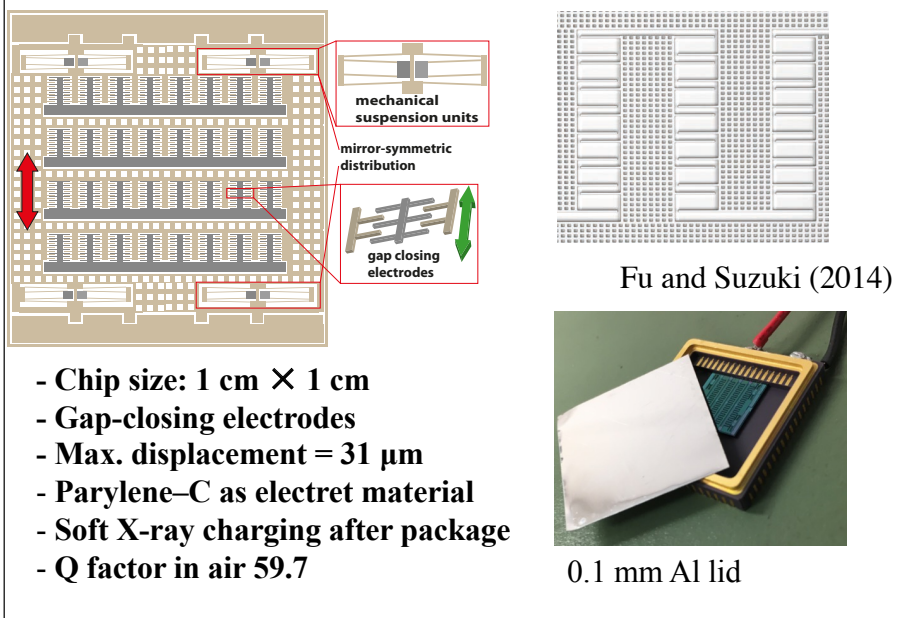
- Wavelength 0.1~10 nm
- X-ray energy 3 – 9.5 keV
- In-situ photoionization
- ✓ Charging after packaging
- ✓ Charging through narrow gaps



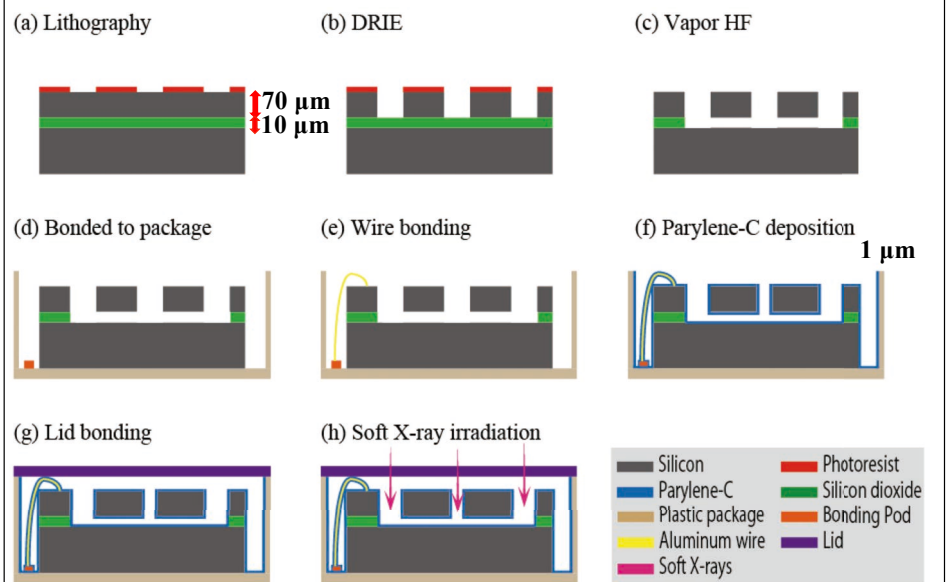
Hagiwara et al., Trans. IEEE, DEI (2012)

Kim et al., PMEMS 2014

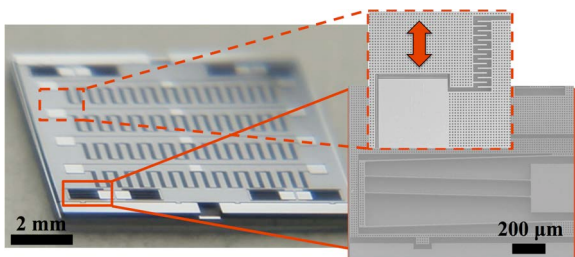
Electret EH with Comb Drives



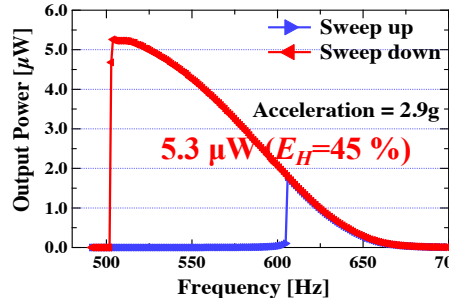
Process Flow



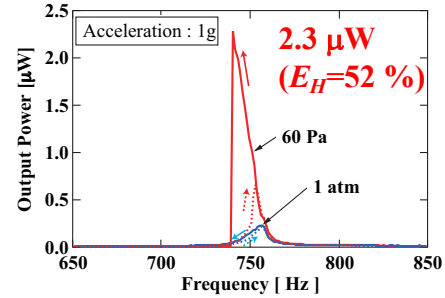
MEMS Electret EH with Comb Drive



Chip size: 1 cm × 1 cm
720 fingers pairs
Max. displacement = 31 μm

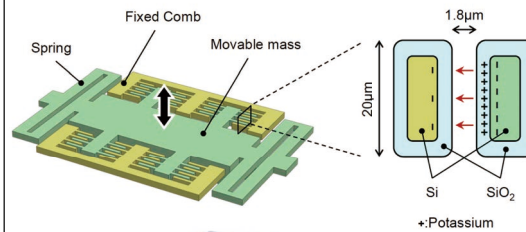


Kim & Suzuki, 2016

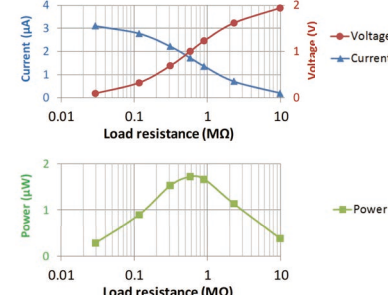


Kim and Suzuki, 2016

MEMS Electret Generator with K-doped SiO₂ Electret

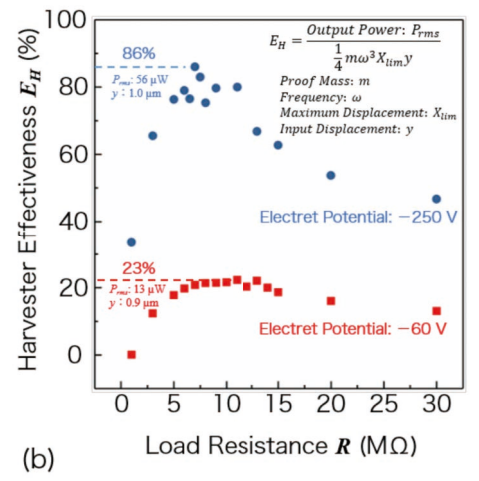
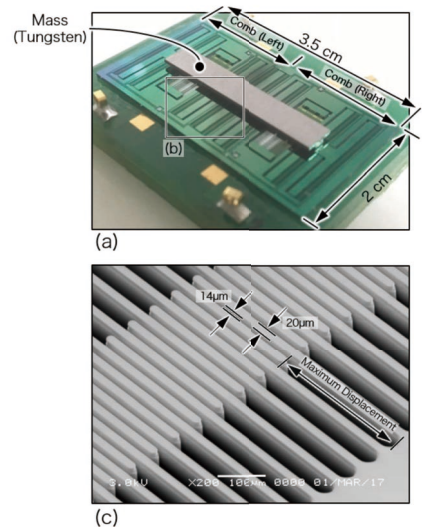


K-doped SiO₂ electret
Bias-Temperature process @500°C, 200V
Surface potential 100V



Ashizawa et al., PowerMEMS 2015

MEMS Electret Generator with K-doped SiO₂ Electret

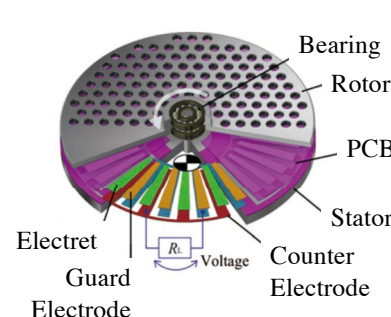


120 Hz, 0.057 G

K-doped SiO₂ electret
Bias-Temperature process @500°C

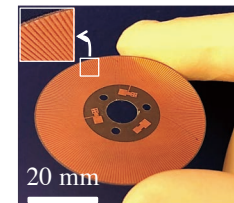
Honnma et al., 2017

PCB-based Rotational Electret EH₅₉



Electret

- ✓ CYTOP EGG
- ✓ Surface potential: ~900V
- ✓ Spun onto PCB and cured at 200 °C



Rotor

Glass-fiber-reinforced PCB

Minimize thermal deformation in curing Electret



Miyoshi et al. IEEE MEMS 2017

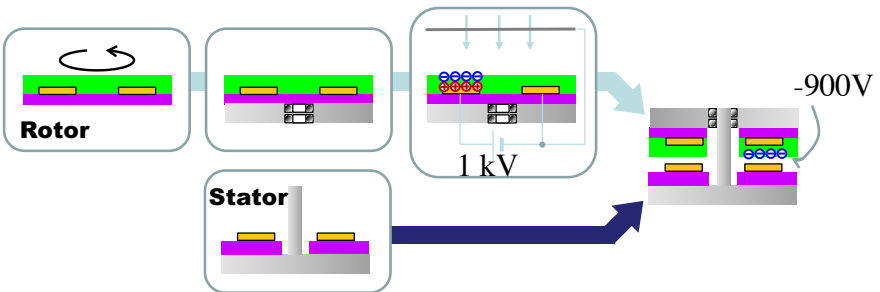
Stator

Low-permittivity PCB ($\epsilon=2.4$)

Reduce parasitic capacitance for higher output power



PCB-based Rotational Electret EH₆₀



CYTOP EGG on
PCB

bonding
between PCBs
and stainless
rotor/stator

charge electret by
soft X-ray

Hagiwara et al.,
2012

1. Coating
CYTOP EGG on
PCB

2. Bonding
between PCBs
and stainless
rotor/stator

3. Charging
charge electret by
soft X-ray

4. Assembling
only by fitting bearing to axis!

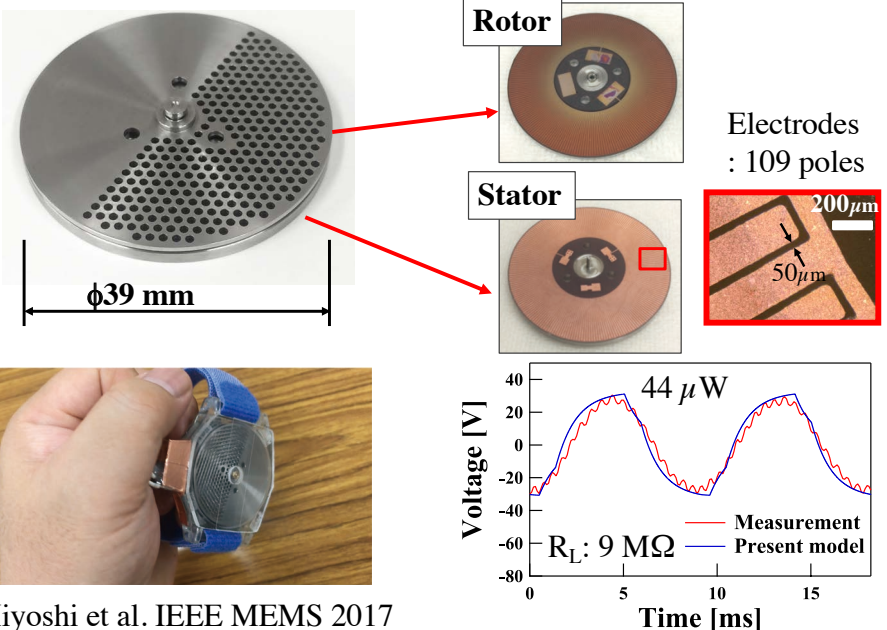
1. Coating
CYTOP EGG on
PCB

2. Bonding
between PCBs
and stainless
rotor/stator

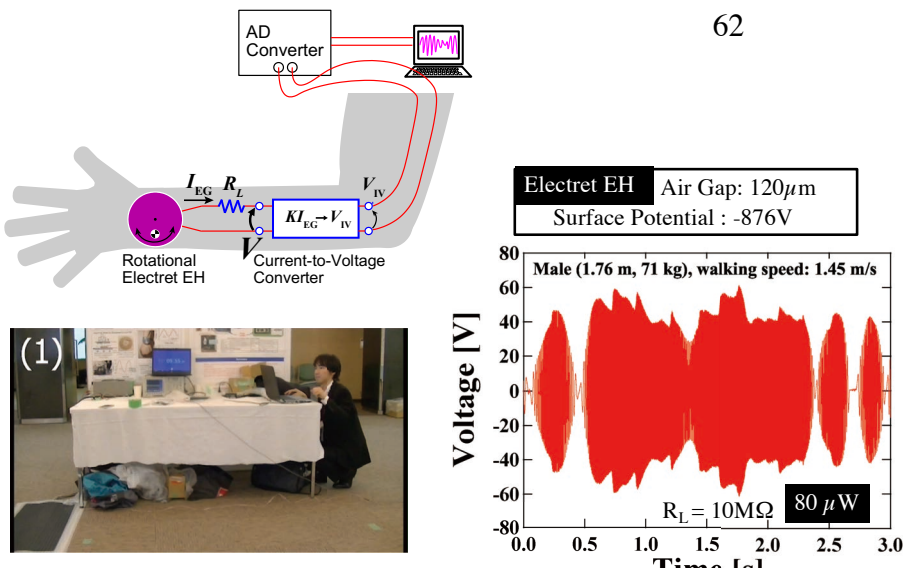
3. Charging
charge electret by
soft X-ray

4. Assembling
only by fitting bearing to axis!

PCB-based Rotational Electret EH



Power Generation during Walking



Miyoshi et al. IEEE MEMS 2017

Contact Charging (Triboelectric Generator)

